

## SYNTHESIS OF A<sup>III</sup> NITRIDES NANOPARTICLES BY AMMONOLYSIS OF COMPLEX FLUORIDE PRECURSORS

KLÍMOVÁ Kateřina<sup>1</sup>, BOUŠA Daniel<sup>1</sup>, HUBER Štěpán<sup>1</sup>, LUXA Jan<sup>1</sup>, SEDMDUBSKÝ David<sup>1</sup>,  
MARYŠKO Miroslav<sup>2</sup>, BRÁZDA Petr<sup>2</sup>, SOFER Zdeněk<sup>1</sup>

<sup>1</sup>University of Chemistry and Technology Prague, Department of Inorganic Chemistry, Prague, Czech Republic, EU, [Katerina.Klimova1@vscht.cz](mailto:Katerina.Klimova1@vscht.cz)

<sup>2</sup>Institute of Physics of the ASCR, v.v.i., Prague, Czech Republic, EU

### Abstract

All III nitrides are crucial materials for current micro- and opto-electronic devices. We present a the simple and scalable synthesis of A<sup>III</sup> nitrides including gallium nitride and indium nitride nanoparticles by rapid thermal decomposition of complex gallium fluoride precursors in ammonia atmosphere. The obtained nanoparticles exhibit disc like morphology and are obtained by precursor decomposition within several minutes at high temperatures. The obtained nanoparticles were characterized by SEM, XRD and Raman spectroscopy. The structural characterization shows the presence of defects like nitrogen vacancies within nitride nanoparticles. The magnetic measurements show a paramagnetic behaviour induced by defects. Nanocrystalline GaN was used for preparation of gallium nitride ceramics which was characterized in detail by X-ray diffraction, SEM and TEM microscopy as well as transport measurement.

**Keywords:** A<sup>III</sup> Nitrides, Nanoparticles, Ammonolysis, Gallium nitride

### 1. INTRODUCTION

The nitrides of A<sup>III</sup> group are ones of the most important materials for the construction of modern optoelectronic and microelectronic devices<sup>1</sup>. The large variability of band-gap ranging from 0.7 eV for InN up to 6.2 eV for AlN and the possibility of solid solution synthesis gives an opportunity for construction of light emitting and detecting devices covering a broad range of wavelengths from NIR up to UV-Vis region<sup>2</sup>. These materials were in the forefront of material research due to their unique optical and electronic properties due to its broad application potential. A<sup>III</sup> nitrides are crucial for modern optoelectronic devices like light emitting diodes, laser diodes and also high power transistors<sup>3</sup>. Due to their low sensitivity towards ionizing radiation and tunable band-gap these materials have a unique potential for application in solar cell. Also other application of A<sup>III</sup> nitrides like photocatalytic water splitting were reported<sup>4</sup>. The A<sup>III</sup> nitride based materials are typically prepared by chemical vapor deposition methods in the form of epitaxial layers using MOVPE and MBE methods<sup>5</sup>. These complex methods are crucial for preparation of epitaxial layers and its heterostructures for device construction. The synthesis of A<sup>III</sup> nitride nanoparticles has been reported in literature using various approaches including hydrothermal synthesis, organometallic precursor decomposition and gas phase reactions of gallium with ammonia<sup>6-8</sup>. The synthesis of nitrides from ammonium hexafluorides of gallium and indium were historically used and described in literature, however, long term annealing produces large particles. The rapid thermal annealing in ammonia atmosphere allowed minimization of particle growth and produced a nanostructured material consisting of disc like shaped nanoparticles.

In this work we report synthesis of GaN and InN nanoparticles by rapid thermal annealing and preparation of nanostructured GaN ceramics by SPS method from GaN nanoparticles. The synthesized materials and ceramics were characterized in detail by various microscopic methods including SEM and TEM. The structure and composition was characterized by X-ray diffraction and Raman spectroscopy. The detailed electrical and thermal transport analysis was performed for GaN ceramics.

## 2. EXPERIMENTAL

### 2.1. Materials

Gallium oxide (99.999%) and indium oxide (99.999%) were obtained from Sigma-Aldrich, Czech Republic. Hydrofluoric acid (48%) and ammonium fluoride (99%) were delivered by Lach-ner, Czech Republic. Nitrogen (99.9999%), ammonia (99.9995%) and argon (99.999%) were obtained from SIAD, Czech Republic.

### 2.2. Procedures

The precursors for nanoparticle synthesis, ammonium hexafluorogallate and ammonium hexafluoroindate, was prepared from high purity gallium oxide and indium oxide, respectively. Firstly 10 g of oxide were dissolved in 50 % hydrofluoric acid (50 mL). Subsequently a three times higher amount of ammonium fluoride with respect to stoichiometry was added in the form of saturated aqueous solution. The resulting white suspension was heated in steam bath for two hours and subsequently the precursor was filtered out. The drying was performed in vacuum oven at 70 °C for 48 hours. The entire precursor synthesis was performed in Teflon labware.

The GaN and InN nanoparticles were synthesized in a horizontal quartz reactor equipped with resistive heating furnace and magnetic manipulator with a sample holder. This configuration allowed us to establish an extremely high temperature gradient without disturbing the high purity atmosphere in the reactor. The thermocouple for the process temperature control was positioned in the middle of the quartz reactor, simultaneously monitoring the reaction temperature. The synthesis was performed in a dynamic nitrogen - ammonia atmosphere (equimolar ratio, total gas flow 600 sccm) in the temperature range from 500 °C to 650 °C for InN and 500 °C to 800 °C for GaN. The precursor was inserted in the hot zone of the furnace for time intervals ranging from 150 s to 60 minutes.

### 2.3. Characterization

Morphology of nanoparticles was investigated using scanning electron microscopy (SEM) with a FEG electron source (Tescan Lyra dual beam microscope). Elemental composition determination and mapping were performed using an energy dispersive spectroscopy (EDS) analyzer (X-MaxN) with a 20 mm<sup>2</sup> SDD detector (Oxford instruments) and AZtecEnergy software. To conduct the measurements, samples were placed on a carbon conductive tape. SEM and SEM-EDS measurements were carried out using a 10 kV electron beam. Transmission electron microscopy (TEM) was conducted on a Philips CM120 transmission electron microscope with a LaB<sub>6</sub> cathode operating at 120 kV. The microscope is equipped with a CCD Camera Olympus SIS Veleta with 14 bit dynamical range and with an EDAX SSD detector Apollo XLTW for EDS analysis. An inVia Raman microscope (Renishaw, England) was used for Raman and photoluminescence spectroscopy in a backscattering geometry with an ultra-low noise CCD detector. A DPSS laser (532 nm, 50 mW) and He-Cd laser (325 nm, 22 mW) with a 50x magnification VIS-NIR and 40x magnification UV optimized objective, respectively, were used for the measurements. The instrument was calibrated using a silicon reference which provided the typical peak position at 520 cm<sup>-1</sup> and a resolution of less than 1 cm<sup>-1</sup>. To ensure a sufficiently strong signal and to avoid radiation damage of the samples, laser power output used for these measurements ranged from 0.1 to 10 mW. Thermal stability was analyzed by simultaneous thermal analysis (STA). DTA and TG curves were recorded simultaneously on a Linseis STA PT1600 apparatus at a heating rate of 10 °C.min<sup>-1</sup> from ambient temperature to 1000 °C in dynamic argon and synthetic air atmospheres (50 cm<sup>3</sup>.min<sup>-1</sup>). X-ray powder diffraction data were collected at room temperature with a Bruker D8 Discoverer powder diffractometer with parafocusing Bragg-Brentano geometry using a CuK $\alpha$  radiation ( $\lambda = 1.5418 \text{ \AA}$ ,  $U = 40 \text{ kV}$ ,  $I = 40 \text{ mA}$ ). The diffraction patterns were acquired over the angular range 5-80° (2 $\theta$ ).

### 3. RESULTS AND DISCUSSION

#### 3.1. Gallium nitride nanoparticles

The morphology of gallium nitride nanoparticles was observed by SEM which revealed a platelet character with a twinning of crystals. The results show extremely rapid formation of GaN at elevated temperatures. The nanoplatelets have a hexagonal profile with a thickness below 100 nm. The crystal morphology is strongly dependent on the synthesis temperature and for lower temperatures a skeletal habitus of nanoplatelets is often observed. On the other hand, well developed crystals of high purity are formed at 800 °C. The resulting purity is discussed in the following paragraphs. The morphology of GaN nanoparticles is shown in **Figure 1**.

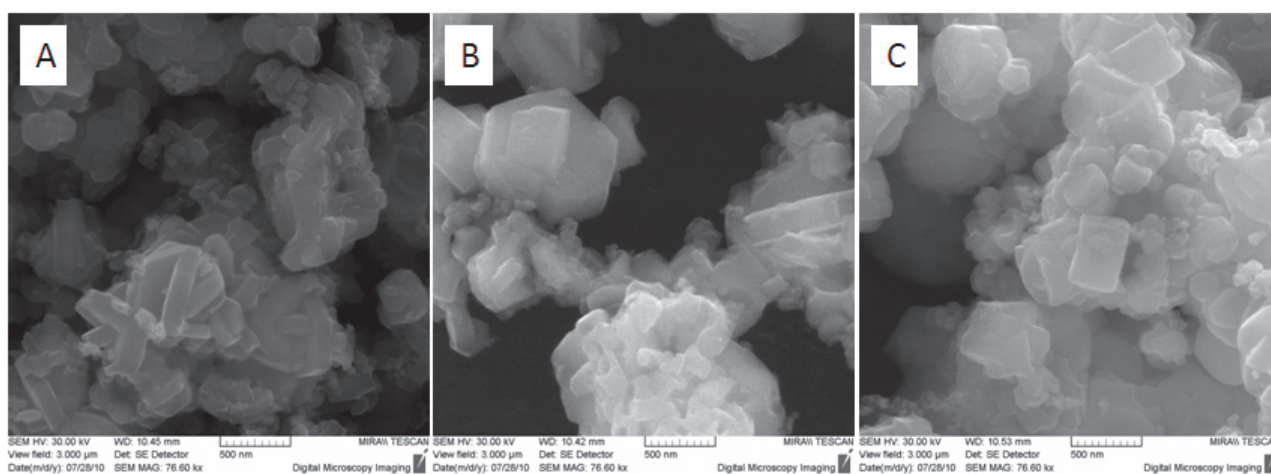


**Figure 1** The morphology of GaN nanoparticles synthesized at 600 °C for 150 s (A), at 700 °C for 150 s (B) and at 800 °C for 150 s

The X-ray diffraction was used to probe of the phase purity of the synthesized materials and a possible presence of unreacted precursors or reaction intermediates. The results show a successful synthesis of GaN by rapid thermal annealing of ammonium hexafluorogallate at 800 °C in 150 second. For the lower temperatures the presence of reaction intermediate, gallium fluoride, was observed. Especially the significant amount of GaF<sub>3</sub> was observed at 600 °C. No significant differences in the nanoparticles structure and no indication of decomposition (e.g. To metallic Ga) were observed for longer annealing times at 800 °C. The results of X-ray diffraction are shown on **Figure 2a**. However, despite no significant differences observed by X-ray diffraction the photoluminescence and Raman spectroscopy show a notable suppression of defect concentration. The GaN nanoplatelets synthesized at 800 °C for 150 s shows only very weak luminescence around 380 nm in comparison with the sample synthesized for 20 minutes. This suggests a substantial improvement of the crystallinity and reduction of defect and dislocation concentration. The photoluminescence maxima correspond to the 3.26 eV which is significantly lower in comparison with epitaxial GaN layers (3.44 eV). This originates from the presence of impurities and defects which strongly influencing the band-gap structure due to the formation of shallow levels. This is also supported by a large broadening of the observed photoluminescence peak. The results of photoluminescence measurements are shown on **Figure 2b**. Raman spectroscopy is also highly sensitive towards the defects and impurities present in the structure. The Raman spectra are dominated by a vibration band at 555 cm<sup>-1</sup> originating from E<sub>2</sub>(high) and E<sub>1</sub>(TO) phonon modes. The shift towards lower wavenumbers compared to single crystal materials originates from defects in the structure. In addition, vibration modes at 250 cm<sup>-1</sup>, 300 cm<sup>-1</sup>, 410 cm<sup>-1</sup> and 706 cm<sup>-1</sup> are observed. The vibration modes observed at 250 cm<sup>-1</sup>, 300 cm<sup>-1</sup> and 410 cm<sup>-1</sup> originate from the defects like nitrogen and gallium vacancies within GaN nanoplatelets. The vibration band at 706 cm<sup>-1</sup> is formed by a

superposition of defects related vibration band with  $A_1(\text{LO})$  phonon mode of GaN. The Raman spectra of samples synthesized at 800 °C for 150 second and 20 minutes are compared on **Figure 2c**. The presence of vacancies was further proved by measurements of magnetization curves at room temperature and at 4.5 K. At room temperature only pure diamagnetic behavior is observed, however at helium temperatures is observed paramagnetic component with a magnetization of 15.5 emu.mol<sup>-1</sup> was identified. The observed paramagnetic behaviour results from high concentration of defects like nitrogen vacancies whose presence was also proofed by Raman spectroscopy. The magnetization curves of GaN nanoparticles synthesized at 800 °C for 20 minutes are shown on **Figure 2d**.

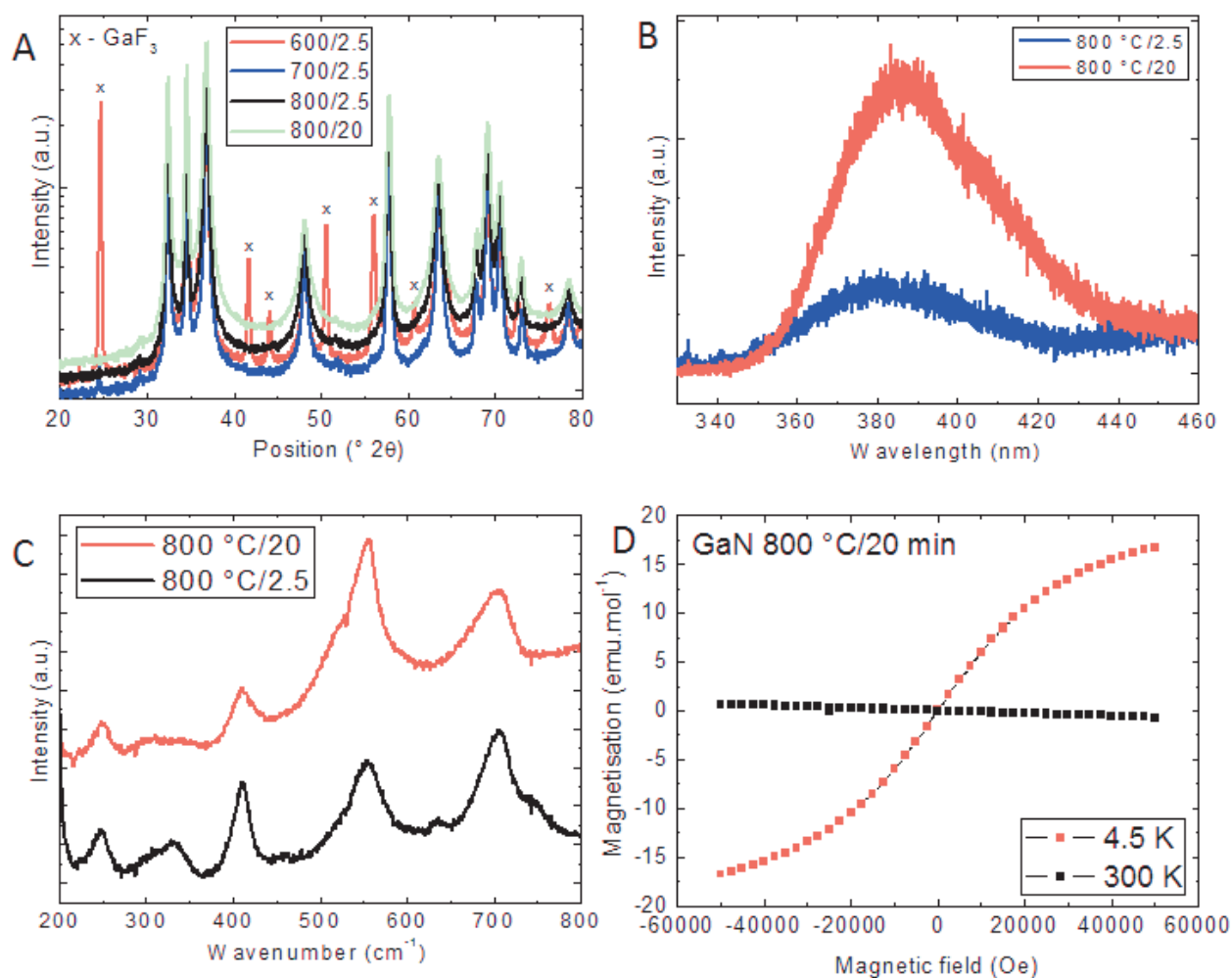


**Figure 2** The X-ray diffraction pattern of GaN nanoparticles synthesized at various temperatures and synthesis time (A), micro-photoluminescence spectra of GaN nanoparticles synthesized at 800 °C (B) and its Raman spectra (C) and magnetization curves of GaN nanoparticles synthesized at 800 °C for 20 minutes

### 3.2. Indium nitride nanoparticles

Indium nitride nanoparticles exhibit platelet morphology with hexagonal shape similar to gallium nitride. However, as clearly seen from the SEM images shown in **Figure 3**, a more defected structure is observed. The individual platelet particles undergo agglomeration, especially for longer synthesis time. The skeletal growth of nanodiscs is observed due to the etching of InN by reaction byproduct, hydrofluoric acid. This is clearly visible for particles synthesized longer time periods.



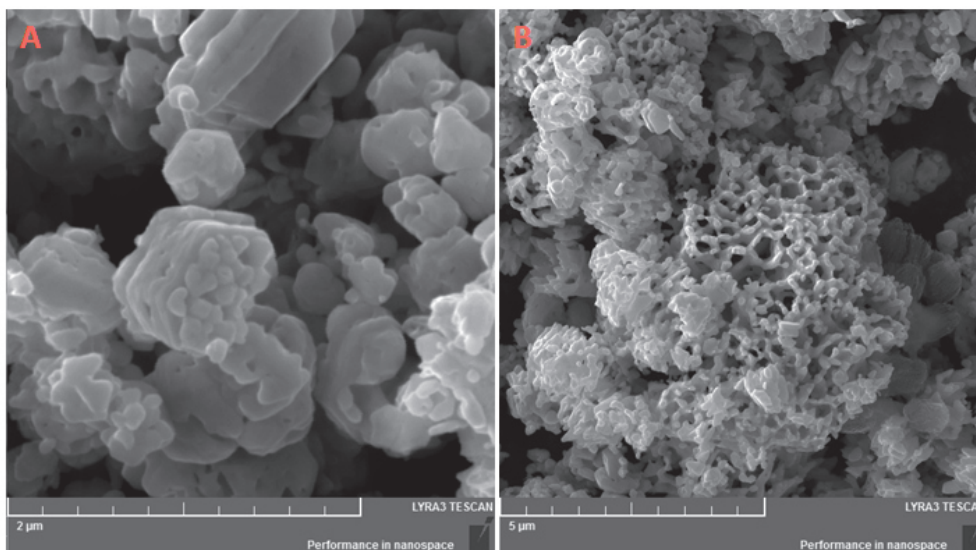


**Figure 3** The morphology of InN nanoparticles synthesized at 600 °C for 30 minutes (A) and 60 minutes (B)

The morphology of InN nanoparticles was further investigated by transmission electron microscopy (see **Figure 4**). All observed nanoparticles exhibit wurtzite structure (P63/mmc symmetry) which was proved by selective area electron diffraction from individual nanoparticles. Visible dark lines inside the nanoparticles indicate the presence of dislocations whose presence was further documented by Raman spectroscopy. Also the surface etching observed by SEM microscopy on nanoparticles synthesized for 60 minutes is clearly visible (**Figure 4c**). The elemental purity was checked by EDS showing the presence of indium together with nitrogen as well as contaminating elements like oxygen and carbon originating from TEM grid.

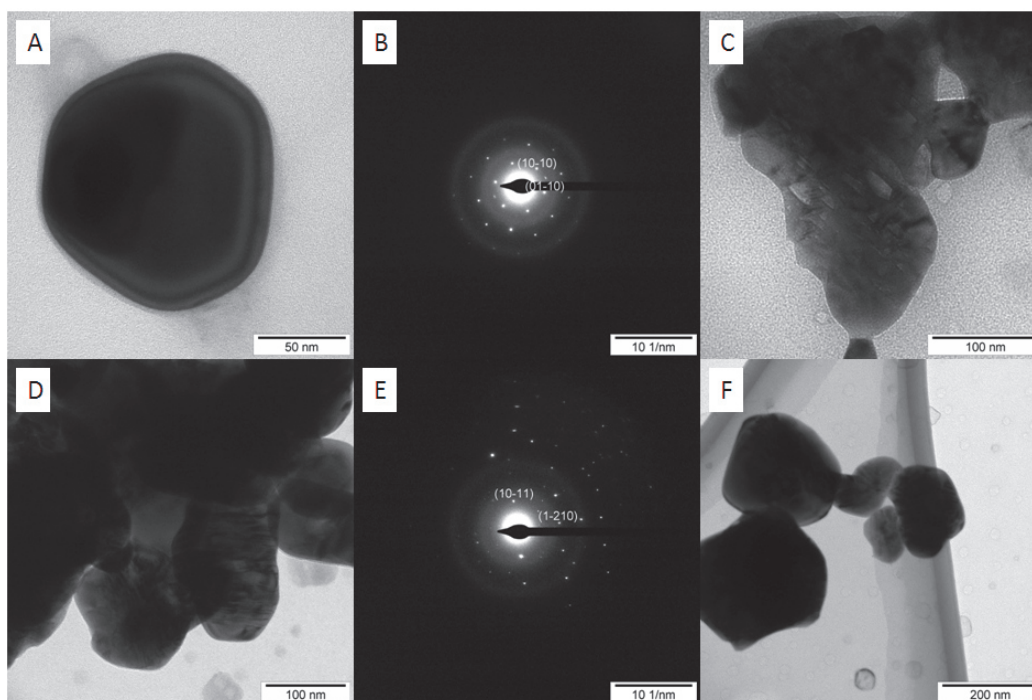


**Figure 4** The TEM images of InN nanoparticles synthesized at 600 °C for 60 minutes (A) with corresponding diffraction image (B) and visible surface etching of nanoparticles (C). The InN nanoparticles synthesized for 30 minutes (D) with corresponding SAED image (E) and agglomerate of individual nanoparticles (F)

The structural characterization shows a strong dependence of phase purity on the synthesis temperature. At temperatures exceeding 600 °C formation of metallic indium due to thermal decomposition is observed. On the other hand, a mixture of indium fluoride-oxide and indium oxide was identified for lower synthesis temperatures. The presence of oxygen which led to a formation of oxides originates from traces of humidity present in InN. The X-ray diffraction patterns are shown on **Figure 5**. The Raman spectroscopy shows significant differences in comparison with high quality epitaxial layers of InN. Apart from the phonon modes originating from wurtzite structure of InN ( $B_1$ ,  $A_1(\text{TO})$ ,  $E_1(\text{TO})$ ,  $E_2(\text{high})$  and  $A_1(\text{LO})$ ) an intensive phonon band around  $310 \text{ cm}^{-1}$  was observed which is associated with defects like nitrogen vacancies.

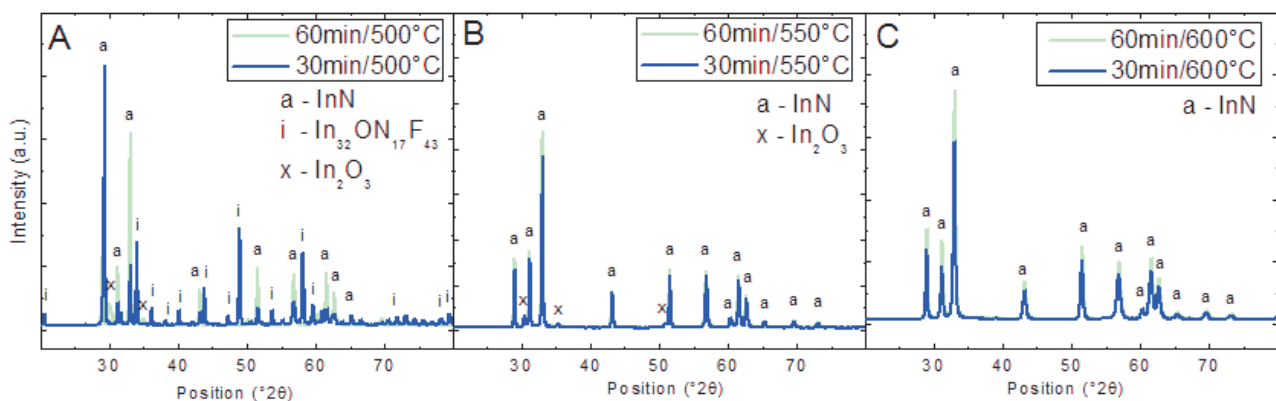


**Figure 5** The X-ray diffraction patterns of InN nanoparticles prepared at 500 °C (A), 550 °C (B) and 600 °C (C)

#### 4. CONCLUSION

The rapid thermal annealing of complex indium and gallium fluoride can be effectively applied for the synthesis of GaN and InN based nanostructures. Due to the hexagonal structure of  $A^{\text{III}}$  nitrides these materials crystallize in the form of hexagonal nanoplates. The morphology is strongly influenced by synthesis conditions, in particular by temperature and time of the synthesis. The formation of GaN was observed within the periods of time below 5 minutes at 800 °C. The rapid synthesis led to the formation of defects like nitrogen and gallium vacancies, which were proved by Raman spectroscopy and magnetic measurements. The reduction of defects concentration can be achieved by extending the time of synthesis without any significant increase of particle size. The synthesis of InN nanoparticles by ammonolysis of complex fluoride precursor has a very narrow temperature region resulting in formation of pure indium nitride with optimal temperature about 600 °C. The synthesis at higher temperatures led to the decomposition of InN, while at lower temperatures incomplete decomposition of precursor was observed. A high concentration of defects and etching of nanoparticles surface was observed by SEM and TEM.

#### ACKNOWLEDGEMENTS

*This work was supported by Czech Science Foundation (GACR No.13-20507S) and by specific university research (MSMT No 20-SVV/2016).*

#### REFERENCES

- [1] DAVIS, R. F., III-V nitrides for electronic and optoelectronic applications. *Proceedings of the IEEE* 1991, 79 (5), 702-712.
- [2] MORKOC, H.; STRITE, S.; GAO, G.; LIN, M.; SVERDLOV, B.; BURNS, M., Large-band-gap SiC, III-V nitride, and II-VI ZnSe-based semiconductor device technologies. *Journal of Applied Physics* 1994, 76 (3), 1363-1398.

- [3] NAKAMURA, S.; CHICHIBU, S. F., *Introduction to nitride semiconductor blue lasers and light emitting diodes*. CRC Press: 2000.
- [4] MAEDA, K.; DOMEN, K., Photocatalytic water splitting: recent progress and future challenges. *The Journal of Physical Chemistry Letters* 2010, 1 (18), 2655-2661.
- [5] ŠIMEK, P.; SEDMIDUBSKÝ, D.; KLÍMOVÁ, K.; MIKULICS, M.; MARYŠKO, M.; VESELÝ, M.; JUREK, K.; SOFER, Z., GaN: Co epitaxial layers grown by MOVPE. *Journal of crystal growth* 2015, 414, 62-68.
- [6] YOSHIMURA, M.; BYRAPPA, K., Hydrothermal processing of materials: past, present and future. *Journal of Materials Science* 2008, 43 (7), 2085-2103.
- [7] GILLAN, E. G., Synthesis of nitrogen-rich carbon nitride networks from an energetic molecular azide precursor. *Chemistry of materials* 2000, 12 (12), 3906-3912.
- [8] ŠIMEK, P.; SEDMIDUBSKÝ, D.; KLÍMOVÁ, K.; HUBER, Š.; BRÁZDA, P.; MIKULICS, M.; JANKOVSKÝ, O.; SOFER, Z., Synthesis of InN nanoparticles by rapid thermal ammonolysis. *Journal of nanoparticle research* 2014, 16 (12), 1-11.